Kirsch et al. J Glycom Lipidom 2012, S2 DOI:
DOI: 10.4172/2153-0637.S2-005

Journal of Glycomics & Lipidomics

Research Article Open Access

Ceramide Profiles of Human Serum Gangliosides GM2 and GD1a exhibit Cancer-associated Alterations

Stephan Kirsch[1], Jamal Souady[1], Michael Mormann[1,2], Laura Bindila[1,3] and JasnaPeter-Katalinić[1,4*]

[1]*Institute of Medical Physics and Biophysics, University of Münster, Germany*
[2]*Institute of Hygiene, University of Münster, Germany*
[3]*Institute of Physiological Chemistry, University Medical Center Mainz, Germany*
[4]*Department of Biotechnology, University of Rijeka, Croatia*

Abstract

Human serum gangliosides were analyzed by nano-HPLC/MS to characterize their glycoforms and ceramide profiles within a single experiment. This unbiased glycosphingolipidomics approach was successfully applied to a set of clinical samples of gastric and pancreatic cancer patients and related control cohorts. Evaluation of acquired data revealed no clear differences with respect to ganglioside glycoforms among the patient groups investigated. However, significant alterations were observed within the ceramide profiles of different ganglioside structures, particularly pronounced for gangliosides GM2 and GD1a. Based on the increase of palmitic acid-comprising structures and the concurrent decrease of stearic acid-comprising ganglioside signals observed for both glycoforms, the ceramide ratio of these signals was applied for discrimination of cancer patients from control sample cohorts. Based on the performance evaluated in statistical analyses, the GM2-related ceramide ratio is proposed as a potential biomarker in particular for pancreatic cancer. Although further validation is required to determine its capability for cancer detection in mass screenings and its applicability for clinical routine, the data presented here support a promising perspective for applications.

Introduction

Various kinds of cancer, such as pancreatic and gastric carcinomas, are associated with high mortality rates that significantly increase with the disease progression at the time of diagnosis [1]. Due to the lack of clear clinical symptoms caused by the gastrointestinal types of cancer only few patients are diagnosed at early stages of the disease. Accordingly, there is an obvious demand for early diagnostic markers to increase survival rates and enable development of new treatment strategies. Glycoconjugates in general have been associated with tumor development since it was discovered, that they are often expressed as onco-developmental antigens [2]. In fact, a significant number of approved cancer biomarkers are glycoproteins being monitored in the blood for their application in diagnosis, prognosis and/or therapy selection of different types of cancer [3]. Although there is growing evidence that glycosphingolipids (GSLs) play an important role in tumor biology, they are not used yet as tumor markers. The qualitative and quantitative analysis of GSLs in routine set-up lags far behind other types of glycoconjugates or biomolecules, which limited so far their interrogation as biomarker candidates and subsequent validation. GSLs are expressed by almost all mammalian cells and consist of a polar glycan chain attached to a nonpolar ceramide moiety. The carbohydrate chain is free for interactions in the extracellular space, while the ceramide portion anchors the GSLs within the outer leaflet of the cell membrane [4]. Being involved in many developmental and cell-signalling processes [5] GSLs are also known to exhibit altered expression due to cancer development. In particular gangliosides, sialylated GSLs, are over expressed in many tumors [6] or exhibit alterations of certain structural elements such as an increased α2-6-sialylation [7] or elevated fucosylation associated with the metastatic potential of a tumor [8].

Being inserted in the plasma membrane, GSLs can be released from their host cell and taken up by another one or by a carrier protein such as blood lipoproteins [9]. This process is referred to as shedding and uptake and is observed for lipid-anchored molecules in general [10]. Gangliosides released in such processes were reported to have various *in vivo* effects, eg. a reduction of an immune response [11-13], a decreased threshold for angiogenic signaling [14] and an enhanced response on epidermal growth factors [15]. Accordingly, shed gangliosides are assumed to promote tumor growth and consequently influence prognosis of the disease. Due to this biological context gangliosides could be feasible biomarkers especially as shedding can affect not only the tumor microenvironment but also serological levels of GSLs. Being well accessible for sample collection the use of blood, serum or plasma is the source of choice for disease monitoring. Several studies already demonstrated increased levels of GSL-bound sialic acid in the serum of patients suffering from mammary carcinoma [16], colorectal cancer [17], and melanoma [18]. Targeted monitoring of single ganglioside structures in cancer patient sera revealed increased concentrations of GM3 and GD3 in the presence of melanoma [19] and elevated levels of GD2 in context of retinoblastoma [20]. Typically, the studies so far were either focused on the total ganglioside amount and accordingly, revealed no information about particularly overexpressed GSL-species, or were based on immunological interactions and consequently performed in a targeted manner with low-throughput, monitoring only a few GSL-species being postulated a priori as "tumor-associated". In order to study serological GSL changes in patients suffering from pancreatic and gastric cancer we employed a recently developed method based on nano-high performance liquid chromatography (nano-HPLC) coupled to electrospray ionization mass spectrometry (ESI-MS) for GSL detection and structural elucidation [21]. This LC/MS approach enables an unbiased monitoring of a broad spectrum of ganglioside structures with increased throughput. Moreover the analytical setup allows the discrimination of isobaric/isomeric analyte

***Corresponding author:** Jasna Peter-Katalinić, Department of Biotechnology, University of Rijeka, RadmileMatejčić 2, 51000 Rijeka, Croatia, E-mail: jasnapk@biotech.uniri. hr

Received October 10, 2012; **Accepted** December 26, 2012; **Published** December 28, 2012

Citation: Kirsch S, Souady J, Mormann M, Bindila L, Peter-Katalinić J (2012) Ceramide Profiles of Human Serum Gangliosides GM2 and GD1a exhibit Cancer-associated Alterations. J Glycomics Lipidomics S2: 005. doi:10.4172/2153-0637.S2-005

species differing with respect to their glycan chain composition as well as determination of ceramide profiles of individual GSL-glycoforms.

Materials and Methods

Reagents

Sample preparation and analysis were performed using LC/MS grade acetonitrile, methanol (Merck, Germany), chloroform, and water (Sigma-Aldrich, Germany). Ammonium acetate (Merck, Germany), Tris, and $CaCl_2$ (Sigma-Aldrich, Germany) were of analytical grade.

Serum samples

Serum samples were collected from patients suffering from gastric carcinoma and pancreatic adenocarcinoma while serum from healthy individuals and patients suffering from non-malignant diseases of the stomach and the pancreas served as a control. Demographic data of patient cohorts are summarized in table 1. Due to the difference in mean age of the control patient group compared to diseased patient cohorts, all disease-associated differences observed in our data were investigated for any correlation with age to exclude an association to aging processes. All sera were collected and provided by RNTECH (Bucharest, Romania). Samples and patient data were collected and stored in accordance with the guidelines of the local ethical committee, compliant with corresponding European regulations.

Sample preparation

For lipid extraction serum aliquots of 300 µl were freeze dried and reconstituted in 1.3 ml of chloroform/methanol/water (30/60/8, v/v/v). Homogenized solutions were sonicated, centrifuged and supernatants were transferred to new vials while the extraction was repeated for the remaining pellets. The obtained extracts were combined and evaporated. Co-extracted phospholipids were depleted by phospholipase C digest. For this purpose, samples were reconstituted in 600 µl digest buffer containing 10 mMTris, 10 mM CaCl2 and 2.5 U *Bacillus cereus* phospholipase C (Sigma-Aldrich, Germany) and incubated over night at 37°C. Further sample preparation involved two steps of solid-phase extraction (SPE). Reversed-phase SPE was performed with Sep-Pak C18 chromatography material (Waters, France) packed into glass cartridges to column volumes (CV) of 250 µl. After column equilibration, the aqueous digest solutions were applied to the cartridge. The flow-though was reapplied twice in order to ensure efficient binding of analytes. After a washing step with 6 CV of water, GSLs were eluted with 3 CV of methanol. Eluates were evaporated and reconstituted in 600 µl chloroform. The second step of SPE was performed with Iatrobead silica chromatography material (Macherey-Nagel, Germany) packed to CV of 200 µl. Following column equilibration, sample solutions were applied and collected flow-through fractions were reapplied twice in order to enhance analyte binding. Cartridges were washed with 3 CV of chloroform and chloroform/methanol (9/1, v/v), respectively. The elution of analytes was performed in four steps using (A) 3 CV chloroform/methanol (2/1, v/v), (B) 3 CV chloroform/methanol (1/2, v/v), (C) 3 CV chloroform/methanol (1/4, v/v), and (D) a combined step of 3 CV methanol and 3 CV methanol/water (4/1). All fractions were evaporated and reconstituted in 40 µl of methanol. C-fractions contain predominantly gangliosides and were used for following nano-HPLC/MS analysis while A-and B-fractions comprised a set of neutral serum GSLs (data not shown). The applied nomenclature of GSLs follows the recommendations of the IUPAC-IUB Joint Commission of Biochemical Nomenclature [22].

Nano-HPLC

Chromatography was performed with an Ultimate 3000 system (Dionex, Germany) equipped with a nanoscale (75 µm×100 mm, 5 µm) TSK gel amide 80 column (Alltech Grom GmbH, Germany). For nano-HPLC analysis the samples were dissolved in acetonitrile/methanol (7/3, v/v) and injected to the column in an amount corresponding to 1.5 µl of serum. Separation of GSLs was carried out by a linear gradient from 5 mM ammonium acetate in acetonitrile/methanol (99/1, v/v) to 5 mM ammonium acetate in methanol/water (8/2, v/v) as reported previously [21]. The eluate was flow-through admitted to MS analysis via a sheathless interface involving coated silica emitters (New Objective, MA, USA) with an inner diameter of 15 µm.

Mass spectrometry

MS analyses were performed in negative ion mode by a quadrupole time-of-flight (QTOF) mass spectrometer equipped with a nano electrospray ion source (Micromass, UK). Experiments were carried out using electrospray voltages in the range of 1.5-2.0 kV and a sampling cone potential of 60 V while a desolvation gas stream of 150 l/h was applied.

Data processing and statistical analysis

MS data acquisition and processing was performed with the MassLynx software (Micromass, UK). Extracted ion chromatograms (EIC) of detected GSL-ions were generated for individual patient samples and used for subsequent statistical analysis. To normalize data and reduce run-to-run variation absolute intensities were converted into percentage intensities relative to the sum of all monitored ganglioside signals.

The non-parametric Mann-Whitney-U test was chosen for statistical evaluation given that most of the detected GSL-signals showed no Gaussian-/normal-distribution within the different patient groups. Curves for receiver operating characteristics (ROC) were generated to investigate the capability of serum GSL signals for identification of cancer patients and their discrimination from control

Patient group	Number	Gender		Age (Mean ± SD)	UICC Cancer stage/ type of benign disease
		Female	Male		
Control (CTR)	38	28	10	30.19 ± 4.4	--------
Pancreatic Cancer (PAN)	17	5	12	59.97 ± 8.86	IA (2), IB (5), IIA (3), IIB (7)
Gastric Cancer (STO)	35	8	27	63.86 ± 8.27	IB (10), II (8); IIIA (6), IIIB (4), IV (7)
Benign diseases pancreas (BP)	8	4	4	54.69 ± 14.45	pancreatitis (7), serous cyst (1)
Benign diseases stomach (BS)	10	2	8	59.01 ± 14.47	stromal tumor (4), active ulcer (3), chronic gastric ulcer (1), gastric schwannoma (1), inflammatory fibroid polyp (1)

Table 1: Demographic data of investigated patient groups. Given are the numbers of patient samples and gender, average and standard deviation for age, subgroups of patients differing in type of benign disease or in cancer stage classified according to the Union of International Cancer Control (UICC).

sample cohorts. All statistical analyses were performed with the PASW statistics 18 (SPSS Inc., IL, USA) software.

Results

Serum gangliosides

It has long been elucidated that neutral GSLs such as monohexyl- and lactosylceramide as well as globo-series GSLs comprise about 80% of the total serum GSL amount and the remaining 20% represent acidic ganglioside structures [23], i.e. GM3, GM2, GD3, GD1a, GD1b and GT1b with GM3 being the most abundant among these ganglioside species [24,25]. Also sialylated nLc4Cer [24] and GM1 [26] were documented to be present at minor concentrations. However, little is known about the ceramide heterogeneity of individual gangliosides. To generate a primary comprehensive list of serum gangliosides we performed nano-HPLC/MS analysis of ganglioside solutions purified from serum of a control volunteer (cf. Materials and Methods). EICs generated for the most intense signal in the ceramide pattern of each detected ganglioside molecular species (Figure 1A) illustrate the relative abundance of individual gangliosides. Gangliosides LC/MS separation was mainly influenced by the length of the glycan chain and the number of included sialic acids. Less polar GSLs such as GM3 (*m/z* 1151.74) and GM2 (*m/z* 1382.86) comprising of three and four carbohydrates, respectively, eluted with low retention times, while the last eluting ganglioside (*m/z* 1707.13, doubly charged) was composed of 16 carbohydrates. This structure represents the most complex GSL that we found in human serum and was to our knowledge for the first time detected in human serum. A few *m/z*-values gave rise to two EIC peaks. As shown previously, such elution profiles originate from a stronger retention of α2-6-sialylated gangliosides compared to α2-3-sialylated isoforms and/or from differences in fucosylation [21]. In case of GD1 ions at *m/z* 917.49, which do not match one of these structural motifs, separated analytes were identified as GD1a (44 min) and the differentially sialylated isoform GD1b (46 min) by tandem-MS analyses (data not shown). With respect to detected ceramide profiles two different subgroups of analytes can be discriminated. Palmitic acid (C16:0)-containing ceramide represents the most abundant lipid structure in almost all serum gangliosides. For GM2 (*m/z* 1382.86), GD1 (*m/z* 917.49) and GT1 (*m/z* 1074.05) structures however, the stearic acid (C18:0)-containing ceramide is the most abundant. Associated mass spectra are displayed for the predominant ganglioside species of each group, GM3 and GD1a, in figure 1B and 1C, respectively. GM3 species contain a large set of different fatty acids ranging from C12:0 to C24:0 within their ceramide moieties where C16:0-ceramides give rise to the most intense signals, followed by C24:1, C18:0, C22:0 fatty acid-comprising structures. In contrast, GD1a exhibits a ceramide profile with fatty acid chain lengths varying between C16:0 and C24:1 where the stearic acid-containing ceramide structure is most dominant. A complete list of GSL-related ions detected in nano-HPLC/MS analysis of human serum gangliosides is given in table 2 along with retention times and structural assignments. In general the serum ganglioside composition as derived from our analysis concurs very well with the data published in literature so far. Yet, the serological GSL profile is furthered particularly with respect to the ceramide pattern occurring among each ganglioside structure. Assignment of structures to the neolacto-or ganglio-series was based on immunostaining data obtained in a parallel study. In this context, also GM1a could be identified although at lower levels as compared to its isobaric structures of $IV^{3/6}$Neu5Ac-nLc4Cer (data not shown). The detected amounts of GD3 could not be monitored in an appropriate way due to the coeluting impurities covering a close *m/z*-range. Data derived within the screening of patient samples revealed a huge intensity variation, and accordingly we decided not to consider GD3-related signals for data normalization or statistical analysis.

Reproducibility

Having a comprehensive map of human serum gangliosides we proceeded to search for changes associated with the onset of cancer. LC/MS protocols for quantitative screening in different sample set would require the application of internal standards for accurate quantification. However, synthetic GSLs of similar structures and length as the serum GSLs are not routinely produced and available, and therefore the use of internal standards is currently compromised. Accordingly, we performed relative quantitation and normalized our data by calculating the percentage value for individual ions based on the sum of all monitored ganglioside signals (Table 2). To investigate the capability of this relative quantitation approach six identical serum aliquots that were pooled from serum samples of ten control volunteers were analyzed. GSLs were purified from each aliquot separately; subsequent nano-HPLC/MS analysis was performed in triplicates. Run-to-run variation was evaluated based on standard deviation of triplicates. Sample-to-sample variation was deduced from standard deviations of triplicate mean values for each investigated sample aliquot. The latter

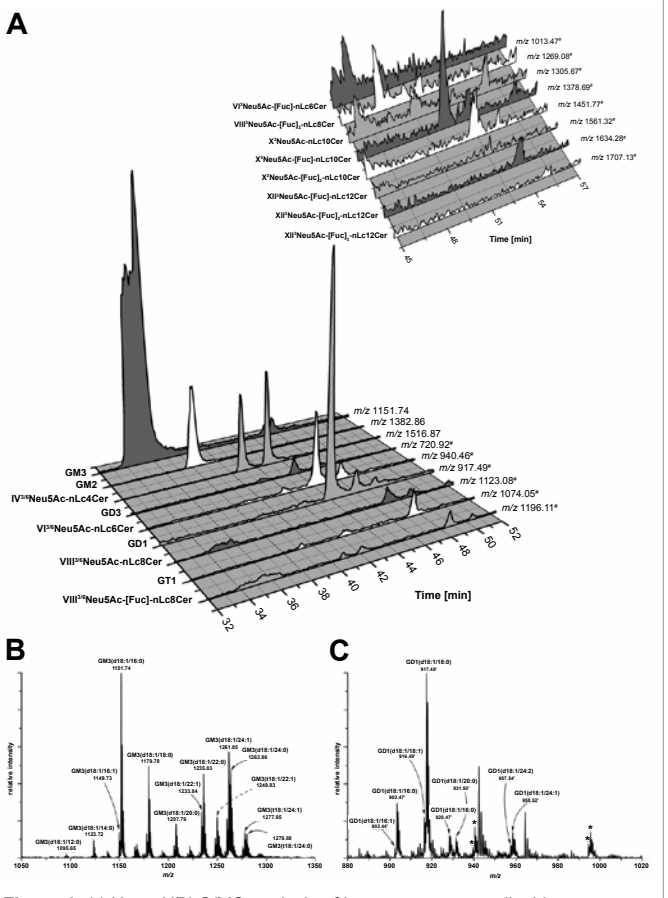

Figure 1: (-) Nano-HPLC/MS analysis of human serum gangliosides.
(A) Display of extracted ion chromatograms (EIC) calculated for the most intense signal in the ceramide pattern of individual ganglioside glycoforms. Insert zooms into a set of less abundant analyte ions (upper line), a detailed list of detected ions is given in Table 2.
(B) Mass spectrum of GM3 ions eluting at min 35.
(C) Mass spectrum of GD1a ions corresponding to an elution time of 44 min. doubly charged ions are marked by#, asterisks indicate partially coeluting VI^3Neu5Ac-nLc4Cer species.

m/z-value (exp.)	*m/z*-value (theo.)	Ion type	Retentiontime [min]		Structure assignment
			1. Peak	2. Peak	
833.56	833.52	$[M-H]^-$	31.26	—	
835.54	835.53	$[M-H]^-$	31.81	—	PI(34:1)
857.54	857.52	$[M-H]^-$	31.07	—	PI(36:4)
859.55	859.55	$[M-H]^-$	31.09	—	PI(36:3)
861.56	861.55	$[M-H]^-$	31.15	—	PI(36:2)
883.55	883.53	$[M-H]^-$	30.99	—	PI(38:5)
885.59	885.55	$[M-H]^-$	30.97	—	PI(38:4)
899.57	899.52	$[M-H]^-$	31.05	—	PI(h38:5)
901.56	901.54	$[M-H]^-$	30.97	—	PI(h38:4)
909.59	909.55	$[M-H]^-$	30.99	—	PI(40:6)
917.56	917.61	$[M-H]^-$	30.95	—	PI(40:2)
571.31	571.29	$[M-H]^-$	34.66	—	LysoPI(16:0)
595.31	595.29	$[M-H]^-$	34.64	—	LysoPI(18:2)
597.33	597.30	$[M-H]^-$	34.50	—	LysoPI(18:1)
599.35	599.32	$[M-H]^-$	34.50	—	LysoPI(18:0)
619.33	619.29	$[M-H]^-$	34.39	—	LysoPI(20:4)
1095.65	1095.64	$[M-H]^-$	35.72	—	GM3(d18:1/12:0)
1123.72	**1123.67**	**$[M-H]^-$**	**35.61**	**—**	**GM3(d18:1/14:0)**
1137.70	1137.65	$[M-H]^-$	35.48	—	GM3(t18:1/14:1)

1149.73	1149.69	– [M-H]	35.54	—	GM3(d18:1/16:1)
1151.74	**1151.71**	**– [M-H]**	**35.50**	—	**GM3(d18:1/16:0)**
1165.74	1165.69	– [M-H]	35.54	—	GM3(t18:1/16:1)
1167.75	1167.70	– [M-H]	36.38	—	GM3(t18:1/16:0)
1177.75	1177.72	– [M-H]	35.40	—	GM3(d18:1/18:1)
1179.78	**1179.74**	**– [M-H]**	**35.40**	**—**	**GM3(d18:1/18:0)**
1193.78	1193.72	– [M-H]	35.40	—	GM3(t18:1/18:1)
1205.77	1205.75	– [M-H]	35.29	—	GM3(d18:1/20:1)
1207.79	**1207.77**	**– [M-H]**	**35.29**	**—**	**GM3(d18:1/20:0)**
1219.77	1219.73	– [M-H]	35.42	—	GM3(t18:1/20:2)
1221.79	1221.75	– [M-H]	35.15	—	GM3(t18:1/20:1)
1233.84	1233.78	– [M-H]	35.20	—	GM3(d18:1/22:1)
1235.83	**1235.80**	**– [M-H]**	**35.20**	**—**	**GM3(d18:1/22:0)**
1247.82	1247.76	– [M-H]	35.12	—	GM3(t18:1/22:2)
1249.83	1249.78	– [M-H]	35.16	—	GM3(t18:1/22:1)
1257.82	1257.79	– [M-H]	35.25	—	GM3(d18:1/24:3)
1259.83	1259.80	– [M-H]	35.18	—	GM3(d18:1/24:2)
1261.85	**1261.82**	**– [M-H]**	**35.12**	**—**	**GM3(d18:1/24:1)**
1263.86	1263.83	– [M-H]	35.11	—	GM3(d18:1/24:0)
1275.82	1275.80	– [M-H]	35.20	—	GM3(t18:1/24:2)

1277.85	1277.81	$[M-H]^-$	36.02	—	GM3(t18:1/24:1)
1279.88	1279.83	$[M-H]^-$	35.98	—	GM3(t18:1/24:0)
1291.83	1291.79	$[M-H]^-$	35.25	—	GM3(t18:1/h24:2)
1293.82	1293.81	$[M-H]^-$	35.08	—	GM3(t18:1/h24:1)
1295.86	1295.82	$[M-H]^-$	36.54	—	GM3(t18:1/h24:0)
1354.84	**1354.79**	**$[M-H]^-$**	**38.17**	**—**	**GM2(d18:1/16:0)**
1368.84	1368.76	$[M-H]^-$	38.06	—	GM2(t18:1/16:1)
1380.84	1380.80	$[M-H]^-$	38.09	—	GM2(d18:1/18:1)
1382.86	**1382.82**	**$[M-H]^-$**	**38.11**	**—**	**GM2(d18:1/18:0)**
1396.83	1396.81	$[M-H]^-$	38.06	—	GM2(t18:1/18:1)

Table 2: Acidic lipid species detected by (-) nano-HPLC/MS analysis of purified ganglioside fractions corresponding to 1.5 µl human serum of a control volunteer patient. Analyte species printed in bold were monitored within the complete set of investigated samples. Asterisks indicate a subset of ions that was not employed for data normalization since low signal intensity hampered their reproducible detection even within the control group.

is depicted in figure 2 for each monitored ganglioside glycoform where intensities of different ceramide structures attached to the same glycan chain were summed for the diagram. Standard deviations are indicated by error bars and relative standard deviations are given by numbers on top of each column. The data displayed clearly demonstrate a good reproducibility of high abundant ganglioside structures varying in a range of about 15% of the mean value while relative standard deviations of less intense ganglioside signals dramatically increase to values of up to 90%. Also the data for run-to-run variation revealed very similar values (data not shown). In both cases the increase of relative standard deviation could be associated mainly to varying background signals of the corresponding spectra that hampered the detection of minor components. If such effects could be prevented, even the monitoring of less abundant structures seems to be possible under well-controlled experimental conditions. Nevertheless, the screening of the other serum gangliosides is straightforward since their signals are not significantly affected by variable background signals. In summary we can conclude the feasibility of our label-free method to generate accurate and reproducible results.

Serum ganglioside levels and ceramide profiles

Since it is known that tumor cells often over express single ganglioside structures we first investigated if ganglioside serum levels correlate with the onset of cancer. For higher reproducibility the major focus of this study was set to the top 10 abundant ganglioside glycoforms. Signal intensities of different ceramide containing ganglioside ions were summed and screened for statistically significant differences. However, statistical analysis revealed only a few minor alterations among the investigated groups (Figure 3), while in total the displayed set of major serum ganglioside constituents remained at a constant level, independent from the disease status. Being only of low statistical significance, these alterations were not suited to discriminate all five patients groups. Since only minor disease-associated changes occurred in terms of ganglioside glycoform levels we decided to focus on the ceramide pattern of the analyzed gangliosides. Differential analysis of data revealed in this case an increase of palmitic acid-containing ceramide structures in serum of cancer patients compared to the non-diseased control group, whereas especially stearic and behenic acid (C22:0)-containing structures exhibited an opposite effect. Remarkably, changes were limited to few ganglioside glycoforms and among them differentially pronounced. Ceramide profiles of GM3, IV^3Neu5Ac-nLc4Cer, and IV^6Neu5Ac-nLc4Cer revealed significant but minor changes (data not shown). By contrast, GD1a (Figure 4A) C16:0-ceramide containing species showed an increase of 40% in case of the pancreatic cancer group while sera of gastric cancer patients exhibited an increase of about 15% relative to the non-diseased control group. The reverse effect was observed for C18:0-ceramides where abundances were reduced by about 20% and 10% in the pancreatic and gastric cancer patient sera, respectively. Relative abundances of C20:0 and C24:1-ceramide comprising GD1a species remained unaffected. Similarly for GM2 (Figure 4C), the C16:0-ceramide structures were more elevated in the pancreatic (63%) and gastric (23%) cancer patient group compared to controls. Control sera of benign diseased patient groups showed a similar trend, though the differences were in both cases less pronounced compared to the corresponding cancer patient group. Based on the association observed for palmitic and stearic acid comprising species, the ratio of measured intensities for every sample was calculated. As documented by boxplots in figure 4B and

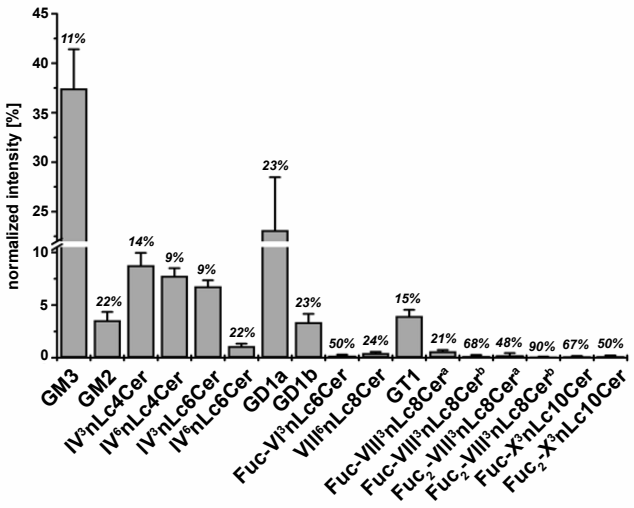

Figure 2: Method Reproducibility. Normalized intensities of gangliosides detected in pooled samples from serum of ten control volunteers. Mean values and standard deviations refer to the sum of monitored ganglioside signals among each glycoform.
Superscribed letters indicate the first (a) and second (b) eluting isoform in case of isobaric structures.

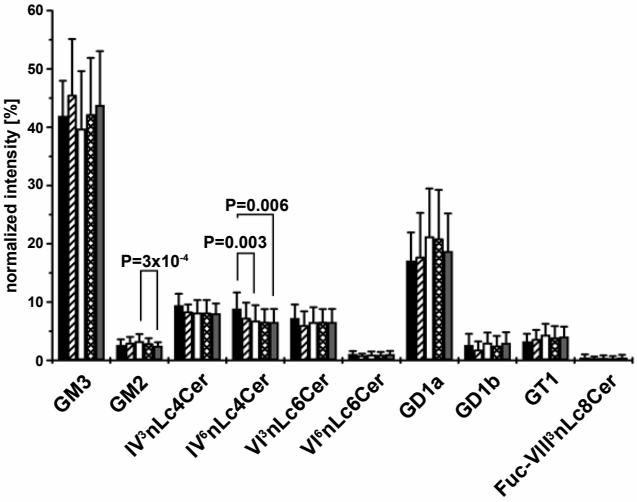

Figure 3: Normalized serum ganglioside levels of ten most abundant ganglioside glycoforms. Mean values and standard deviations refer to the sum of monitored ganglioside signals among each glycoform. Patient groups are represented by the columns as follows: pancreatic cancer (black), benign pancreatic diseases (striped), non-diseased controls (white), benign gastric diseases (checked), gastric cancer (grey).

4D for GD1a and GM2, respectively, both gangliosides exhibit a very similar trend. The control groups show the lowest CerC16:0/CerC18:0 ratio while elevated values among the investigated cancer groups can be observed. Particularly samples obtained from pancreatic cancer patients feature a much broader spectrum of values, demonstrating a high individual variability of this sample cohort. P-values displayed within the diagrams demonstrate highly significant differences between control patients and the cancer patient groups. To further evaluate the significance of the ceramide ratio for cancer detection and consequently its applicability for cancer diagnosis a ROC-analysis was carried out. Therefore, the positive identification of cancer patients based on GM2-and GD1a-related CerC16:0/CerC18:0 ratios were evaluated in reference to the non-diseased control group only (Figure 5A), as well as the combined set of relevant benign and non-diseased control patients (Figure 5B). As demonstrated by the diagrams the GM2-related values revealed a much better performance for detection of both types of cancer when compared to the GD1a-related data. In addition, CerC16:0/CerC18:0-based cancer detection was clearly superior for the pancreatic cancer where area under the curve (AUC) values of up to 96% for the dissection of malignant and non-diseased control patients was reached. Considering additionally the benign diseased control group an AUC value of 93% could be obtained for the GM2-related ceramide ratio. Although the detection of gastric cancer was less efficient for both investigated data sets, AUC values of 85% could still be achieved for GM2.

Discussion

Serum ganglioside composition

A great portion of serum glycosphingolipids originates from shedding processes at various cell types. Consequently this pool of biomolecules originates from different sources of the body [10]. Unfortunately, the tissue or cell type origin of single ganglioside constituents in the serum cannot be elucidated yet. Though, based on the ganglioside composition of cells that are in the close contact with blood, such as blood cells and endothelial tissues, it can be hypothesized that shedding at these cells predominantly affect GSL levels in serum. Both, erythrocytes [19] and endothelial cells [27,28] mainly comprise GM3 and IV^{3}Neu5Ac-nLc4Cer while leucocytes were found to contain a broad spectrum of singly sialylated neolacto-series gangliosides ranging from GM3 up to XIV^{3}Neu5Ac-nLc14Cer [29,30]. The cerebrospinal fluid that is connected to the blood via the lymphatic system [31] could be another source of serum ganglio-series

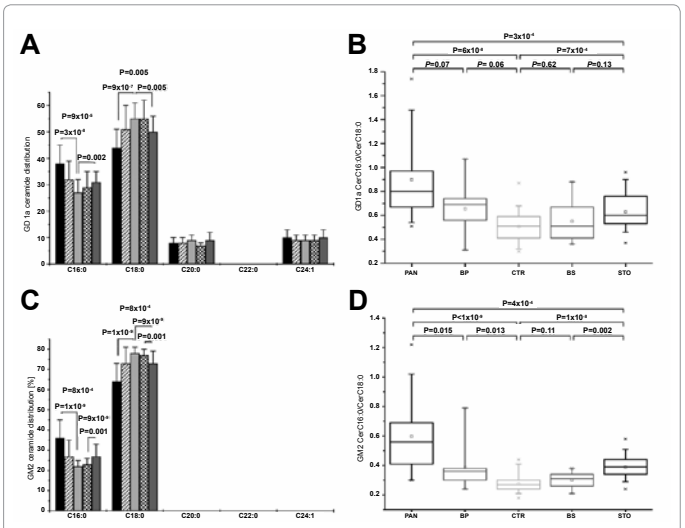

Figure 4: Ceramide profiles and CerC16:0/CerC18:0 ratios of serum gangliosides GD1a and GM2. Ceramide signals are normalized based on the sum of all structures detected among (A) GD1a and (C) GM2 for each sample. CerC16:0/CerC18:0 ratios of (B) GD1a and (D) GM2 of individual patients are displayed as boxplots. Patient groups are represented as follows: pancreatic cancer (black/PAN), benign pancreatic diseases (striped/BP), non-diseased controls (white/CTR), benign gastric diseases (checked/BS), gastric cancer (grey/STO). Error bars indicate standard deviations. P-values displayed in the upper panel of each diagram (panels A and C only for P≤0.01) were obtained by the non-parametric Mann-Whitney-U test.

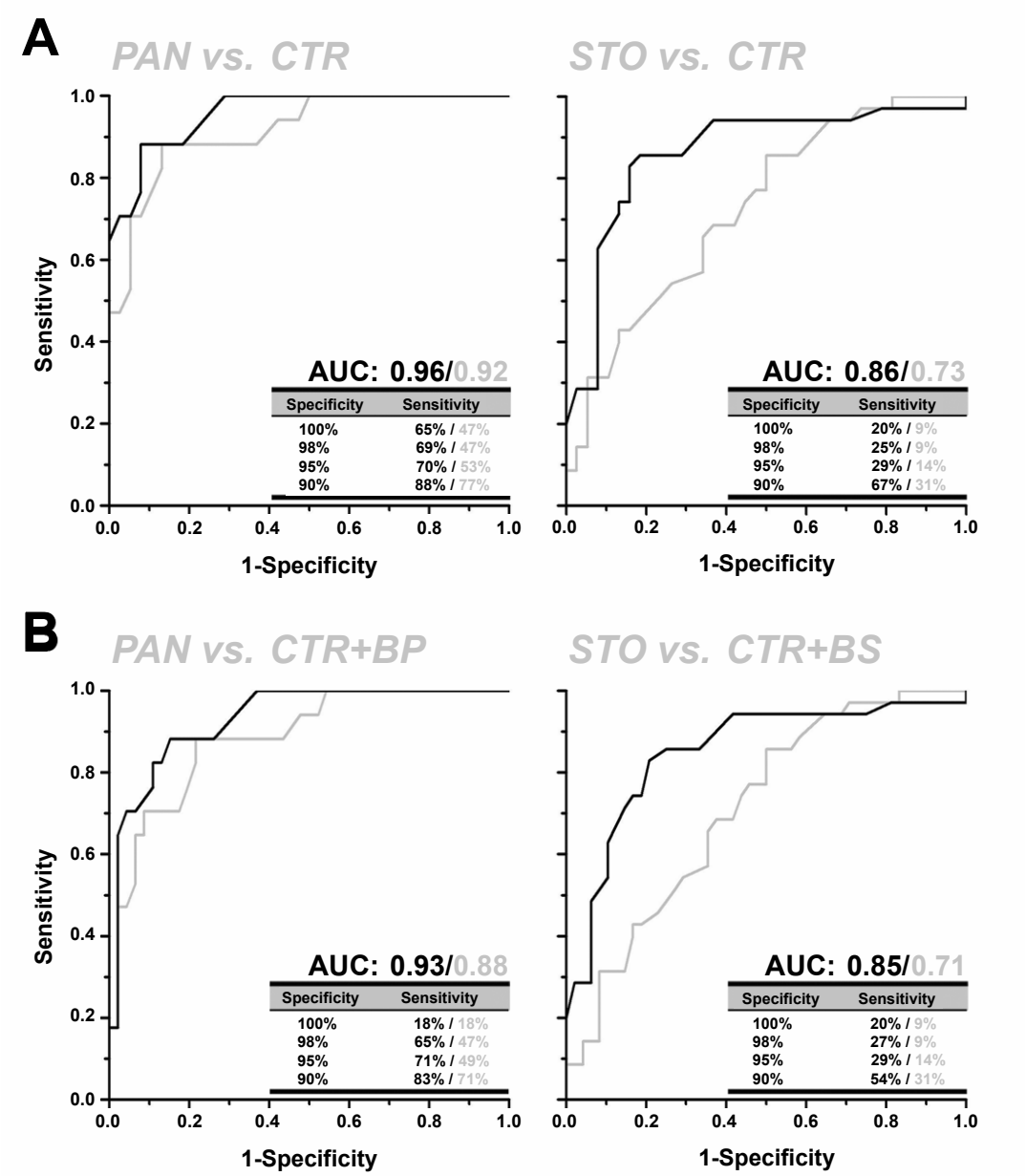

Figure 5: ROC-curves for identification of pancreatic and gastric cancer patients based on GM2-and GD1a-related ceramide ratios. (A) ROC-plots for identification of pancreatic (PAN) or gastric cancer patients (STO) combined in data sets with non-diseased controls (CTR). (B) ROC-curves for identification of pancreatic or gastric cancer patients combined in data sets with non-diseased controls and patient cohorts suffering from benign diseases of the pancreas (BP) and the stomach (BS), respectively. Curves were calculated for GM2-(black lines) and GD1a-related CerC16:0/CerC18:0 ratios (grey lines).

gangliosides as it contains especially GD1a, GD1b, GT1b, and GQ1b [32]. Due to their reduced anchoring potential within the membrane preferably lipids with short chain fatty acids are shed [33]. Concordant with this fact, our data demonstrate that serum gangliosides exhibit a relatively high abundance of palmitic and stearic acid and only to a minor extend long chain fatty acids. Interestingly, ceramide profiles vary among the different ganglioside structures detected in serum. In case of GD1a, GD1b, GT1, and GM2 most intense signals derive from structures containing stearic acid in their ceramide moiety while in all other profiles the most abundant species contain palmitic acid. The fact that especially neuronal tissues highly express Cer(d18:1/18:0) structures [34] might support the hypothesis that the corresponding gangliosides are originally shed from neuronal tissues and are subsequently transported into the blood. Still, other tissue types exhibiting a similar ceramide synthase (CerS) expression could represent alternative sources, and accordingly concerted efforts will be needed to elucidate the serum GSL sourcing.

Cancer-associated alterations

Although tumors can induce strong alterations of serum ganglioside glycoform levels [35] data generated in the course of our current study revealed no obvious differences among the five patient groups. Due to our analytical set-up we could obtain a relative quantitative response, in which a general increase of the serum levels of all ganglioside

species cannot be monitored. However, a parallel study on a similar set of patient samples employing semi-quantitative immunostaining of thin-layer separated gangliosides being consistent with our current results did not indicate such an effect (data not shown). Although total serum levels remained unchanged, unambiguous alterations in the ceramide profiles of different gangliosides could be evidenced (Figure 4). Relative abundances of C16:0-ceramide-comprising structures were elevated while those of C18:0-ceramides significantly reduced in cancer patient samples. Similar effects have been observed for the ceramide composition in human head and neck squamous carcinoma cells (HNSCC) [36] and breast cancer tissues [37]. A proposed mechanism for these changes has been associated to the expression the ceramide synthases CerS6 and CerS1 and their effect on ER-stress mediated apoptosis via activation of caspase-3 [38]. In this context, CerS6/C16:0-ceramide downregulation and CerS1/C18:0-ceramide induction was found to similarly increase programmed cell death *in vitro* and *in vivo*. Moreover increased C18-ceramide levels were found to correlate with the lymphovascular invasion and the formation of nodal metastases in HNSCC tumors [39] and thus evaluated as serum biomarkers in a recent phase II trial to monitor a chemotherapeutic response [40]. These effects were described for free ceramide structures, however, similar changes among GSL structures were to our knowledge not investigated so far. In fact, many GSL studies are still focused on the glycan chain composition only although it is well known that the ceramide portion can reveal important biological information [41]. The strong association of observed changes in ceramide profiles to gangliosides GD1a and GM2 could be related to the tissue characteristics of both investigated tumors. Representing adenocarcinomas, both tumor types derive from glandular and thus epithelial tissues. GM2 has been reported to be expressed on a variety of epithelial tissues including those of the pancreas and the stomach [42]. In addition, also the presence of GM2 in the majority of corresponding carcinomas could be evidenced. Although GD1a expression was less detailed investigated it was detected in different carcinomas or derived cell lines [43-45]. Accordingly, this association to epithelial cells could suggest that similar alterations might also occur among other (adeno) carcinomas. The ROC-analysis revealed a good capability of the GM2-related ceramide ratio for detection of pancreatic cancer. Although many biomarkers proposed so far exhibit a higher performance for the discrimination of control patients and pancreatic cancer patients, their major drawback is the lack of feasibility to discriminate between malignant and benign diseased patients [46,47]. In our study such effects were clearly less pronounced. However, due to the relatively small set of patient samples analyzed in this study further validation is necessary in order to determine the feasibility of the GM2-and GD1a-related ceramide profiles for clinical use.

Conclusions

In this current study of human serum no alterations of ganglioside glycoforms with respect to cancer and cancer type, were observed at a significant level. The unbiased nano-HPLC/MS approach used for the analysis of serum gangliosides enabled however the identification of cancer-related changes within the ceramide profiles of several ganglioside structures. To our knowledge this is the first study documenting serum level alterations of GSL fatty acid substitution with cancer. Based on the performance evaluated in ROC-analysis the GM2-related ceramide ratio represents a potential biomarker for pancreatic cancer. Discrimination of pancreatic cancer patients and non-diseased control volunteers could be accomplished at 92.1% sensitivity and 88.2% selectivity. Taking into account also benign diseased control patients' performance dropped slightly to 89.1% sensitivity and 84.8% selectivity which is still superior to other biomarkers proposed so far. In the case of gastric cancer the GM2-related ceramide ratios revealed less specificity for cancer patient detection that renders an application for tumor detection alone unlikely.

Grant support

The study was financially supported by the European Union GLYFDIS project (project no. LSHB-CT-2006-037661, to J.P.K.) and the Deutsche Forschungsgemeinschaft within the Sonderforschungsbereich 492 (project Z2). S.K. is a fellow of the German National Academic Foundation (Studienstiftung des Deutschen Volkes).

References

1. Jemal A, Siegel R, Ward E, Hao Y, Xu J, et al. (2008) Cancer statistics, 2008. CA Cancer J Clin 58: 71-96.
2. Feizi T (1985) Demonstration by monoclonal antibodies that carbohydrate structures of glycoproteins and glycolipids are onco-developmental antigens. Nature 314: 53-57.
3. Ludwig JA, Weinstein JN (2005) Biomarkers in cancer staging, prognosis and treatment selection. Nat Rev Cancer 5: 845-856.
4. Prinetti A, Loberto N, Chigorno V, Sonnino S (2009) Glycosphingolipid behaviour in complex membranes. Biochim Biophys Acta 1788: 184-193.
5. Hakomori S (1981) Glycosphingolipids in cellular interaction, differentiation, and oncogenesis. Annu Rev Biochem 50: 733-764.
6. Marquina G, Waki H, Fernandez LE, Kon K, Carr A, et al. (1996) Gangliosides expressed in human breast cancer. Cancer Res 56: 5165-5171.
7. Distler U, Souady J, Hülsewig M, Drmić-Hofman I, Haier J, et al. (2008) Tumor-associated CD75s- and iso-CD75s-gangliosides are potential targets for adjuvant therapy in pancreatic cancer. Mol Cancer Ther 7: 2464-2475.
8. Kannagi R (1997) Carbohydrate-mediated cell adhesion involved in hematogenous metastasis of cancer. Glycoconi J 14: 577-584.
9. Valentino LA, Ladisch S (1992) Localization of shed human tumor gangliosides: association with serum lipoproteins. Cancer Res 52: 810-814.
10. Lauc G, Heffer-Lauc M (2006) Shedding and uptake of gangliosides and glycosylphosphatidylinositol-anchored proteins. Biochim Biophys Acta 1760: 584-602.
11. Heitger A, Ladisch S (1996) Gangliosides block antigen presentation by human monocytes. Biochim Biophys Acta 1303: 161-168.
12. Caldwell S, Heitger A, Shen W, Liu Y, Taylor B, et al. (2003) Mechanisms of ganglioside inhibition of APC function. J Immunol 171: 1676-1683.
13. Shen W, Falahati R, Stark R, Leitenberg D, Ladisch S (2005) Modulation of CD4 Th cell differentiation by ganglioside GD1a in vitro. J Immunol 175: 4927-4934.
14. Liu Y, McCarthy J, Ladisch S (2006) Membrane ganglioside enrichment lowers the threshold for vascular endothelial cell angiogenic signaling. Cancer Res 66: 10408-10414.
15. Li R, Liu Y, Ladisch S (2001) Enhancement of epidermal growth factor signaling and activation of SRC kinase by gangliosides. J Biol Chem 276: 42782-42792.
16. Kloppel TM, Keenan TW, Freeman MJ, Morré DJ (1977) Glycolipid-bound sialic acid in serum: increased levels in mice and humans bearing mammary carcinomas. Proc Natl Acad Sci USA 74: 3011-3013.
17. Perez CA, Ravindranath MH, Gupta RK, Tollenaar RA, van de Velde CJ, et al. (2002) Serum total gangliosides and TA90-IC levels: novel immunologic markers in colorectal cancer. Cancer J 8: 55-61.
18. Ravindranath MH, Hsueh EC, Verma M, Ye W, Morton DL (2003) Serum total ganglioside level correlates with clinical course in melanoma patients after immunotherapy with therapeutic cancer vaccine. J Immunother 26: 277-285.
19. Portoukalian J, Zwingelstein G, Abdul-Malak N, Doré JF (1978) Alteration of gangliosides in plasma and red cells of humans bearing melanoma tumors. Biochem Biophys Res Commun 85: 916-920.
20. Portoukalian J, David MJ, Gain P, Richard M (1993) Shedding of GD2 ganglioside in patients with retinoblastoma. Int J Cancer 53: 948-951.

21. Kirsch S, Müthing J, Peter-Katalinić J, Bindila L (2009) On-line nano-HPLC/ESI QTOF MS monitoring of alpha2-3 and alpha2-6 sialylation in granulocyte glycosphingolipidome. Biol Chem 390: 657-672.

22. Chester M (1998) IUPAC-IUB Joint Commission on Biochemical Nomenclature (JCBN). Nomenclature of glycolipids--recommendations 1997. Eur J Biochem 257: 293-298.

23. Chatterjee S, Kwiterovich PO (1976) Glycosphingolipids of human plasma lipoproteins. Lipids 11: 462-466.

24. Senn HJ, Orth M, Fitzke E, Wieland H, Gerok W (1989) Gangliosides in normal human serum. Concentration, pattern and transport by lipoproteins. Eur J Biochem 181: 657-662.

25. Kundu SK, Diego I, Osovitz S, Marcus DM (1985) Glycosphingolipids of human plasma. Arch BiochemBiophys 238: 388-400.

26. Ayabe M, Shichijo S, Yokoyama MM (1989) Diagnostic value of ganglioside patterns in plasma of human diseases. J Clin Lab Anal 3: 301-306.

27. Gillard BK, Jones MA, Marcus DM (1987) Glycosphingolipids of human umbilical vein endothelial cells and smooth muscle cells. Arch Biochem Biophys 256: 435-445.

28. Kanda T, Ariga T, Kubodera H, Jin HL, Owada K, et al. (2004) Glycosphingolipid composition of primary cultured human brain microvascular endothelial cells. J Neurosci Res 78: 141-150.

29. Müthing J, Spanbroek R, Peter-Katalinić J, Hanisch FG, Hanski C, et al. (1996) Isolation and structural characterization of fucosylated gangliosides with linear poly-N-acetyllactosaminyl chains from human granulocytes. Glycobiology 6: 147-156.

30. Nimrichter L, Burdick MM, Aoki K, Laroy W, Fierro MA, et al. (2008) E-selectin receptors on human leukocytes. Blood 112: 3744-3752.

31. Veening JG, Barendregt HP (2010) The regulation of brain states by neuroactive substances distributed via the cerebrospinal fluid; a review. Cerebrospinal Fluid Res 7: 1.

32. Trbojevic-Cepe M, Kracun I, Jusic A, Pavlicek I (1991) Gangliosides of human cerebrospinal fluid in various neurologic diseases. J Neurol Sci 105: 192-199.

33. Chang F, Li R, Ladisch S (1997) Shedding of gangliosides by human medulloblastoma cells. Exp Cell Res 234: 341-346.

34. Kadowaki H, Evans JE, McCluer RH (1984) Separation of brain monosialoganglioside molecular species by high-performance liquid chromatography. J Lipid Res 25: 1132-1139.

35. Ladisch S, Wu ZL (1985) Circulating gangliosides as tumor markers. Prog Clin Biol Res 175: 277-284.

36. Koybasi S, Senkal CE, Sundararaj K, Spassieva S, Bielawski J, et al. (2004) Defects in cell growth regulation by C18:0-ceramide and longevity assurance gene 1 in human head and neck squamous cell carcinomas. J Biol Chem 279: 44311-44319.

37. Schiffmann S, Sandner J, Birod K, Wobst I, Angioni C, et al. (2009) Ceramide synthases and ceramide levels are increased in breast cancer tissue. Carcinogenesis 30: 745-752.

38. Senkal CE, Ponnusamy S, Bielawski J, Hannun YA, Ogretmen B (2010) Antiapoptotic roles of ceramide-synthase-6-generated C16-ceramide via selective regulation of the ATF6/CHOP arm of ER-stress-response pathways. FASEB J 24: 296-308.

39. Karahatay S, Thomas K, Koybasi S, Senkal CE, Elojeimy S, et al. (2007) Clinical relevance of ceramide metabolism in the pathogenesis of human head and neck squamous cell carcinoma (HNSCC): attenuation of C(18)-ceramide in HNSCC tumors correlates with lymphovascular invasion and nodal metastasis. Cancer Lett 256: 101-111.

40. Saddoughi SA, Garrett-Mayer E, Chaudhary U, O'Brien PE, Afrin LB, et al. (2011) Results of a phase II trial of gemcitabine plus doxorubicin in patients with recurrent head and neck cancers: serum C_{18}-ceramide as a novel biomarker for monitoring response. Clin Cancer Res 17: 6097-6105.

41. Yin J, Miyazaki K, Shaner RL, Merrill AH Jr, Kannagi R (2010) Altered sphingolipid metabolism induced by tumor hypoxia - new vistas in glycolipid tumor markers. FEBS Lett 584: 1872-1878.

42. Zhang S, Cordon-Cardo C, Zhang HS, Reuter VE, Adluri S, et al. (1997) Selection of tumor antigens as targets for immune attack using immunohistochemistry: I. Focus on gangliosides. Int J Cancer 26: 42-49.

43. Prinetti A, Aureli M, Illuzzi G, Prioni S, Nocco V, et al. (2010) GM3 synthase overexpression results in reduced cell motility and in caveolin-1 upregulation in human ovarian carcinoma cells. Glycobiology 20: 62-77.

44. Ugorski M, Påhlsson P, Dus D, Nilsson B, Radzikowski (1989) Glycosphingolipids of human urothelial cell lines with different grades of transformation. Glycoconj J 6: 303-318.

45. Ravindranath MH, Muthugounder S, Presser N, Selvan SR, Portoukalian J, et al. (2004) Gangliosides of organ-confined versus metastatic androgen-receptor-negative prostate cancer. Biochem Biophys Res Commun 324: 154-165.

46. Simeone DM, Ji B, Banerjee M, Arumugam T, Li D, et al. (2007) CEACAM1, a novel serum biomarker for pancreatic cancer. Pancreas 34: 436-443.

47. Chen R, Crispin DA, Pan S, Hawley S, McIntosh MW (2010) Pilot study of blood biomarker candidates for detection of pancreatic cancer. Pancreas 39: 981-988.